Progress in PHOTOVOLTAICS

PROGRESS IN PHOTOVOLTAICS: RESEARCH AND APPLICATIONS
Prog. Photovolt: Res. Appl. 2015; **23**:428–436
Published online 16 December 2013 in Wiley Online Library (wileyonlinelibrary.com). DOI: 10.1002/pip.2443

RESEARCH ARTICLE

Influence of cracks on the local current–voltage parameters of silicon solar cells

Tobias M. Pletzer[1]*, Justus I. van Mölken[1], Sven Rißland[2], Otwin Breitenstein[2] and Joachim Knoch[1]

[1] RWTH Aachen University, Institute of Semiconductor Electronics, Sommerfeldstraße 24, D-52074 Aachen, Germany
[2] Max Planck Institute of Microstructure Physics, Department 2, Weinberg 2, D-06120 Halle, Germany

ABSTRACT

The existence of cracks in silicon solar cells can drastically reduce the electrical performance of an individual cell and even of an entire photovoltaic module. An in-depth understanding of the influence of cracks on solar cells enables therefore calculations of the crack impact and other following effects on module level. This paper shows a detailed analysis of the electrical influence of cracks with two different spatially resolved methods including global and local current–voltage characteristics. The main influence of cracks is an increased recombination current density in the depletion region, which is clearly shown by spatially resolved dark lock-in thermography measurements with local current–voltage investigation. This increased recombination current density affects further cell parameters such as the efficiency, which is confirmed also by the global current–voltage characteristics. The additionally used ratio image technique based on electroluminescence measurements is in comparison with the local current–voltage method, the more reliable and faster method for the crack detection itself, and allows on cell-level and module-level a continuous inspection of cracks. Copyright © 2013 John Wiley & Sons, Ltd.

KEYWORDS

cracks; electroluminescence; dark lock-in thermography; spatially resolved characterisation; silicon solar cells; local current–voltage parameters

***Correspondence**

Tobias M. Pletzer, RWTH Aachen University, Institute of Semiconductor Electronics, Sommerfeldstraße 24, D-52074 Aachen, Germany.
E-mail: pletzer@iht.rwth-aachen.de

Received 8 July 2013; Revised 20 September 2013; Accepted 22 October 2013

1. INTRODUCTION

Cracks or micro-cracks in silicon (Si) wafers or solar cells can reduce the electrical performance [1] or mechanical stability of cells, which could result in a destroyed cell or decreased output power of photovoltaic (PV) modules. Cracks occur during the solar cell processing due to the stress resulting from particular process steps with high temperatures as well as the mechanical handling of cells in manufacturing or during the transport of solar cells or PV modules. In the case of PV modules, a strong wind load or a heavy snow weight can induce sufficient mechanical stress for crack formation [2].

Electroluminescence (EL) camera based imaging [3] is a well-established measurement technique to identify cracks in solar cells and to characterise cells as well as PV modules in a fast way with high resolution. Furthermore, the preparing of ratio images [1] with EL images before and after crack formation allows a detailed investigation of cracks. Cracks can also be identified with the dark lock-in thermography (DLIT) [4]. The DLIT technique does not provide high resolution but allows a quantitative analysis of cells.

The quantitative analysis of solar cells with DLIT allows the determination of local current–voltage (I–V) data like open circuit voltage (V_{OC}), fill factor (FF) and efficiency (η) in a spatially resolved manner [5,6]. Also, the two-diode model parameters, alias internal cell parameters such as saturation current density of the first diode (J_{01}) linked to the recombination outside the space charge region (SCR), saturation current density of the second diode (J_{02}) linked to recombination within the SCR and parallel (or shunt) resistance (R_P), can be determined with this method. The series resistance (R_S) is obtained according to the so-called recombination current and series resistance imaging method

[7] from an EL-based local voltage image [8]. In this evaluation, the short circuit current density (J_{SC}) is assumed to be homogeneous across the whole cell.

In this paper, we investigate cracks in Si solar cells with two experimental methods, that is, the ratio image technique based on EL imaging before and after crack formation, including global *I–V* data analysis and the DLIT method with the analysis of local *I–V* data. The first method used, which is the ratio image technique, is able to distinguish cracks from the already existing other defect types (grain boundaries or dislocations) in a reliable way. The second method, the DLIT-based local *I–V* data analysis, allows a quantitative investigation and enables the analysis of cracks without a need for images taken before and after crack formation. This local *I–V* analysis is necessary to investigate the effect of cracks on the internal cell parameters and further their influence on the external *I–V* values.

Both methods allow the crack detection, but the field of application can be different. This is discussed in a contrasting juxtaposition, which shows the advantages of each method as well as their limitations. This evaluation allows the selection of the most suitable method for each different defect or crack detection as well as their detailed investigation.

2. EXPERIMENTAL DETAILS

2.1. Sample preparation

Conventionally fabricated screen-printed aluminum (Al) back surface field Si solar cells were used in this study. The cells were processed with solar-grade as-cut multi-crystalline (mc) Si p-type wafers with a boron doping corresponding to 1 Ωcm and a full square sample size of 156.25 cm^2. The wafers were wet-chemically textured and cleaned before the emitter formation in a phosphorus oxychloride ($POCl_3$) diffusion furnace was carried out. Afterwards, the phosphosilicate glass layer was removed, followed by the deposition of a hydrogenated amorphous silicon nitride (a-SiNx:H) passivation and anti-reflection coating layer in a plasma-enhanced chemical vapour deposition chamber. Finally, silver (Ag) contacts on the front and full size Al contacts on the backside of the cells were screen-printed and co-fired in a belt furnace completed by an edge isolation step. The cracks were deliberately introduced in the edge regions of the cells by using a mechanical edge isolation tool (detailed description in Section 2.4).

2.2. Ratio image method based on electroluminescence with global *I–V* data

The ratio image method [1] based on EL imaging needs for the detection of cracks and micro-cracks as well as their effect on cell parameters two different EL measurements. In our case, a typical EL camera with a Si charge coupled device chip was used to take the first image before the crack formation and the second image afterwards. All images were taken at a forward current density of 9.6 mA/cm^2 within a few seconds. The pixel-wise division of these two images before and after crack formation results in a ratio image, which clearly shows, within the limit of the spatial resolution of EL, any kind of crack or other formed defects. The division has, in comparison with the subtraction, the advantages that it is not affected by different emission intensities during the EL measurement. Furthermore, the ratio image is not limited by any other cell effects or defects, which already existed in the cell during the first EL image.

Additionally, illuminated *I–V* curves were taken for the investigated solar cells before and after the crack formation. All *I–V* curves were measured in the Institute of Semiconductor Electronics Aachen at 1000 W/m^2 light intensity, complying with the international standard of the International Electrotechnical Commission 60904. The used system is developed and constructed by the calibration laboratory (CalLab) of the Fraunhofer Institute for Solar Energy Systems Freiburg and has a measurement precision of +/− 1% relative as it is given in the specification of the system. The *I–V* curves allow the calculation of typical cell parameters (J_{SC}, V_{OC}, FF and η) as well as the extraction of the two-diode model values (J_{PH}, J_{01}, J_{02}, R_S and R_P) [9] according to the following equation:

$$J = J_{PH} - \frac{V + JR_S}{R_P} - J_{01}\left(e^{\frac{q(V+JR_S)}{k_B T}} - 1\right) - J_{02}\left(e^{\frac{q(V+JR_S)}{n_2 k_B T}} - 1\right) \quad (1)$$

The external voltage and current density are V and J, respectively. J_{PH} stands for the photo current density, k_B is Boltzmann's constant, n_2 is the ideality factor of the second diode and T is the temperature. The two-diode model parameters can be used to determine the influence of cracks and micro-cracks on the typical solar cell parameters [1].

2.3. Local *I–V* method based on dark lock-in thermography

The investigation of local *I–V* characteristics are performed by DLIT measurements at 10 Hz while biassing with four different voltages of 500, 550, 600 mV and −1 V, which allows the quantitative evaluation of the different saturation current densities with respect to the different used voltages to subsequently solve the two-diode model equation for each pixel. In this way, it is possible to evaluate the different local dark current contributions by the software tool called 'Local I-V' [5] from the Max Planck Innovations GmbH in Munich/Germany, which is based on the mentioned approach. To obtain an overview on the distribution of the recombination-active defects including cracks and to be able to calculate the necessary R_S image by the recombination current and series resistance imaging method [7], EL measurements at 550 and 600 mV were also conducted and evaluated to an image of the local voltage by the tool 'EL-Fit' [8] from the Max Planck Innovations GmbH in Munich/Germany.

All the calculations in 'EL-Fit' as well as in the 'Local I-V' tools are made under the assumption of an injection-independent carrier lifetime, which corresponds to the

ideality factor n_1 of the first diode (diffusion) current of unity [10]. Furthermore, the 'Local I-V' tool allows the determination of local *I–V* characteristics including two-diode model values of the investigated cell for each pixel of the used camera including the calculation of the diffusion (first diode) current density (J_{diff}) and the depletion region recombination current density (J_{rec}) at a particular voltage, for example, 550 mV. The associated equations of J_{diff} and J_{rec} are in the following form:

$$J_{diff} = J_{01}\left(e^{\frac{q\left(V+JR_S\right)}{k_B T}} - 1\right) \tag{2}$$

and

$$J_{rec} = J_{02}\left(e^{\frac{q\left(V+JR_S\right)}{n_2 k_B T}} - 1\right) \tag{3}$$

This $J_{rec}(550\,mV)$ is used instead of J_{02} because of the evaluation procedure of the current density for the second diode with variable ideality factor n_2. For a given magnitude of the recombination current density, the value of J_{02} is strongly (exponentially) influenced by the value of n_2. Both practical experience [4] and theory [11] show that there is a correlation between the magnitude of the recombination current density and n_2. This variation in J_{rec} and n_2 can be many orders of magnitude for a local point of the solar cell. The 'Local I-V' tool is also able to calculate the total current density (J_{tot}) over all currents at a certain voltage, which includes diffusion, recombination and shunt current densities. This value is also used in this work.

For the measurement, the sample was placed on a temperature-stabilised copper chuck and covered by a black foil, and the vacuum provided a good electrical and thermal contact between the sample and the chuck. Additionally, the foil homogenises the emissivity at the surface, which is necessary for the correct quantitative evaluation of the signals measured at the metallization.

2.4. Experimental approach

Typical industrial type mc-Si solar cells as described in Section 2.1 were taken for the investigation in this work. The solar cells were characterised by illuminated *I–V* curve measurements to estimate cell parameters (J_{SC}, V_{OC}, FF and η) followed by the calculation of two-diode model values (J_{PH}, J_{01}, J_{02}, R_S and R_P) [9]. Also, the first EL images for the ratio image calculation (Section 2.2) were taken at this stage.

Afterwards, cracks and micro-cracks were formed by a machine, which is originally used for the mechanical edge isolation of solar cells. A slightly higher pressure of the grinding head allows the controlled formation of cracks without destroying the cells. All cells were investigated again by EL measurements to get the second image for the ratio image calculation. Also, *I–V* curve measurements were performed again to obtain the data for the calculation of the affected global *I–V* characteristics by cracks. In the EL and DLIT imaging tools used here, only macroscopic cracks can be detected.

To calculate the influence of cracks on the local *I–V* characteristics of solar cells, EL and DLIT images were taken as described in Section 2.3. The 'EL-Fit' [8] and the 'Local I-V' tools [5,6] were used to calculate the spatially resolved local *I–V* parameters for each pixel (for example, V_{OC}, FF and η) including two diode-model values such as J_{01}, J_{02} or R_S in each investigated cell.

Both results, from ratio image method and local *I–V* method, together with global *I–V* measurements, were used in a complementary way on a representative sample of the investigation in this work to demonstrate the influence of cracks as well as the differences and advantages of both methods. Thereby, the validity of this investigation is confirmed by similar results obtained from further samples, but these are not shown here for an easier overview.

Finally, the samples were investigated by scanning electron microscopy (SEM) and prepared by the focused ion beam technique for investigation in a high resolution SEM. Both microscopy techniques were used to find out if cracks or micro-cracks are responsible for the *I–V* characteristics of the solar cells in this investigation.

For a comparison to the parameters obtained from the measured *I-V* characteristics, the local parameters of the dark characteristic like J_{01}, J_{02}, and R_P are averaged pixel-wise. In contrast to that the global illuminated *I-V* curve is simulated by summing up all local current densities [6]. Then the global parameters FF, V_{OC}, and η are obtained from the resulting *I-V* curve.

3. RESULTS AND DISCUSSION

3.1. Scanning electron microscopy analysis of cracks

First of all, to clarify the following interpretations of the results depending on the crack types observed in this work, the results of the SEM analysis are discussed. For this purpose, investigated solar cells were cleaved into small pieces containing the crack areas for evaluation in SEM, and previously detected cracks by other investigation techniques (EL ratio and DLIT images) were taken into account. A top view SEM image in Figure 1(a) shows a small segment of a solar cell with a crack, which is observed frequently in this work. The crack begins at the top of the picture and continues down to the bottom, changing the direction in the middle at a grain boundary. The high resolution SEM in Figure 1(b) shows that the width of this crack is well below 1 µm. Note that parts of the cracks generated by the edge isolation (Section 2.4) do not cross the whole wafer thickness but end at the Si-Al interface or sometimes somewhere in the Si material. Therefore, the following discussion is based on the assumption that the *I–V* characteristics are significantly affected by cracks, which are to be seen in SEM images (Figure 1).

DOI: 10.1002/pip

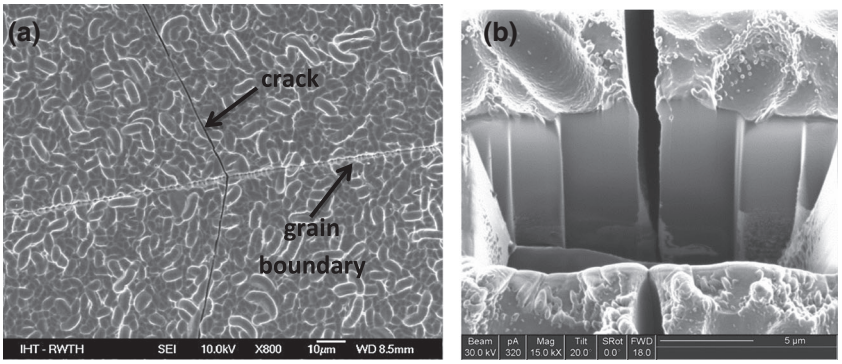

Figure 1. The top view picture (a) is taken by scanning electron microscopy and shows a typical crack, which was formed by mechanical edge isolation and changes the direction at a grain boundary. The cross section picture (b) was taken by a high resolution scanning electron microscopy and shows another similar crack at a focused ion beam groove in a higher resolution.

3.2. Results of the electroluminescence ratio image method

The procedure of the EL ratio image method was described in Section 2.2, and the results are presented here on an exemplary sample. As was shown by van Mölken, *et al.* [1], the stability of this ratio image method is proven with average parameters for different solar cell batches. Figure 2 (a) shows the EL image of the mc-Si solar cell before any crack formation. The dark grey regions represent low material quality, which exhibits a high dislocation density. After the formation of cracks, the image in Figure 2(b) is taken. In comparison with the first image of Figure 2(a), additional cracks are visible but sometimes not easily recognisable and hard to distinguish from grain boundaries or other defects. The slightly darker upper halves of both images (figure (a) and figure (b)) appear to be caused by the settings of the used EL tool. But this phenomenon is in both images identical and therefore not relevant for calculation of the ratio image or the investigation in this work. A decrease in EL intensity of the second image of figure (b) compared with the first image of figure (a), hence a ratio smaller than 1 in the ratio image of figure (c), is equivalent to a decrease of the local minority carrier diffusion length in the bulk under certain assumptions regarding the EL intensity [12]. Therefore, the dark regions in the calculated ratio image in Figure 2(c) correspond to a reduced diffusion length. Moreover, the ratio image shows only the additional defects or artefacts, which were formed during mechanical edge isolation, and no other defects influence the inspection. These are mainly the cracks, which are now clearly visible as dark lines. The cracks enter the cell from the edges because of the formation process. Furthermore, two concentric circles in the middle of the cell are visible (one of them almost not visible). These two circles are surface damages from the sample holder in the mechanical edge isolation machine. Also, contact probes of the EL measurement tool on the busbars are slightly visible because of a minor misalignment during sample positioning. But in any case, cracks are the dominant additional defect type after crack formation. Therefore, any further differences observed in cell parameters such as in the *I–V* measurement results are based on cracks. Regarding the ratio image in Figure 2(c), it can be stated that the diffusion length is reduced locally down to approximately 50% because of the generated cracks.

The results of the illuminated *I–V* curve measurements before and after the crack formation are presented in Table I. Furthermore, the absolute and relative differences of each measured unit are listed in Table I to point out the

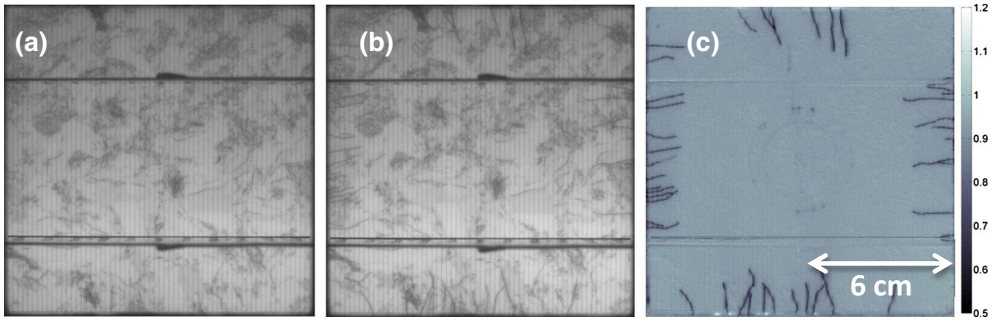

Figure 2. The image (a) shows electroluminescence measurement result before the crack formation and the image (b) after the crack formation. The ratio image is shown in the image (c), where the cracks are clearly visible.

Table I. Solar cell parameters of the investigated mc-Si solar cell determined by illuminated *I–V* curve measurements before and after the formation of cracks as well as the calculated differences.

	J_{SC} (mA/cm^2)	V_{OC} (mV)	FF	η (%)
Before the crack formation	33.1	616.0	0.790	16.11
After the crack formation	32.9	613.5	0.786	15.87
Absolute (and relative) difference because of the crack formation	−0.2 (−0.6%)	−2.5 (−0.4%)	−0.004 (−0.5%)	−0.24 (−1.5%)

influence of cracks on the solar cell parameters. The J_{SC} value decreases by 0.2 mA/cm^2 after the crack formation, which is related to the increased recombination activity of the cracks and also because of a loss of active cell area and a reduced current transport because of possible damage of gridlines. A loss of 2.5 mV is measured for the V_{OC} and indicates that cracks increase the bulk recombination activity, hence they increase J_{01}. A small FF loss of 0.5% relative is also observed as an absolute loss of 0.2% in η, which demonstrates the negative influence of cracks on the solar cell parameters.

For a more detailed analysis, the two-diode model parameters were calculated and listed in Table II. All two-diode model calculations were carried out with a constant value of 2 for n_2 to enable an easier comparison of the data. A variation of n_2 could allow a more exact estimation of the two-diode model parameters, but the variation of n_2 is a local effect and rather difficult to interpret as global value. Furthermore, a drastic change of a two-diode model data due to a crack can be certainly verified with a constant n_2. The loss of 0.2 mA/cm^2 in J_{PH} goes along with the loss in J_{SC}. The observed variations in J_{01} as well as in R_S are insignificant and in an accuracy range of the two-diode model calculation. A different behaviour is observed for J_{02} and R_P. In the case of R_P, the additional mechanical edge isolation is the reason for the increase of 324 Ωcm^2, which is a relative change of 13.4%. It must be taken into account that the determination of R_P could strongly depend on the value of n_2 if a constant or variable value was chosen. A drastic change is observed in J_{02}, with a relative difference of 30.7% and an absolute difference of 9.1 nA/cm^2. This strong increase is caused by the formed cracks and evidences that cracks generated new recombination centres, which are active in the bulk and in the SCR, where the carrier separation occurs. The new recombination centres in the bulk are also responsible for the reduced V_{OC}.

3.3. Results of the local *I-V* method

The 'Local I-V' analyses were performed as described in Section 2.3. Thereby, the corresponding DLIT measurements (not shown here) were used to calculate the spatially resolved images for V_{OC}, FF, η, J_{diff} (550 mV), J_{tot} (550 mV) and J_{rec} (550 mV). Further images of other entities such as J_{SC}, R_S or R_P are not taken into account because of nonrelevance in the case of cracks for this investigation.

In Figure 3, the images of J_{diff} (550 mV), J_{tot} (550 mV) and J_{rec} (550 mV) are shown. The image (a) represents the J_{diff} (550 mV) distribution of the investigated solar cell, which means that all recombination outside the SCR often correlated to bulk recombination. The blue regions suggest a low recombination activity, and the red/yellow regions are highly recombination active regions. There are recombination areas in Figure 3(a), which look similar to lines and correlate with cracks shown in the image (c) of Figure 2. But also further recombination areas in forms of lines can be seen in the image (a) of Figure 3, which correspond to regions of low luminescence in the EL images (see image (b) of Figure 2) but not based on cracks. These non-crack areas are recombination-active grain boundaries or dislocations. A unique correlation between cracks and the J_{diff} (550 mV) image (a) is not observed because of the presence of the grain boundaries, but the correlation to the J_{02} image is better. It is well known that single recombination-active grain boundaries are not leading to measurable J_{02} signals [4]. The reason that the global J_{02} is much stronger increased by the cracks than J_{01} (Table II) is that only J_{01} shows a significant homogeneous contribution, whereas J_{02} is only a local current [4].

The examination of the J_{tot} (550 mV) image of Figure 3(b), which sums up all dark current densities, shows obviously a correlation of high local losses at the position of cracks (compare with Figure 2(c)). Knowing that shunts are not caused by cracks, the J_{rec} (550 mV) image of Figure 3(c) is taken into account, which is preferred for the evaluation at fixed voltage

Table II. Two-diode model values of the investigated mc-Si solar cell calculated from the corresponding *I–V* curves before and after the formation of cracks including the differences.

	J_{PH} (mA/cm^2)	J_{01} (pA/cm^2)	J_{02} (nA/cm^2)	R_S (Ωcm^2)	R_P (Ωcm^2)
Before the crack formation	33.1	0.99	29.6	0.34	2421
After the crack formation	32.9	1.00	38.7	0.34	2745
Absolute (and relative) difference because of the crack formation	−0.2 (−0.6%)	+0.01 (−1 %)	+9.1 (+30.7%)	0 (0%)	+324 (+13.4%)

DOI: 10.1002/pip

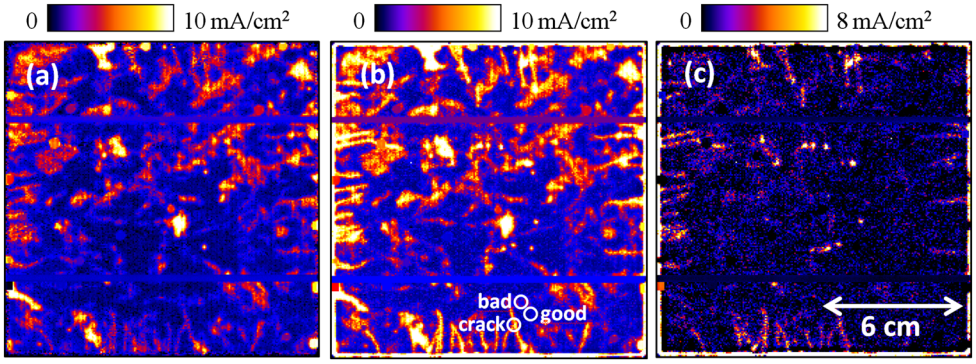

Figure 3. Results of the 'Local I-V' investigation. The image (a) shows an illustration of J_{diff} (550 mV), image (b) of J_{tot} (550 mV) and image (c) of J_{rec} (550 mV). Note the different scaling range in image (c).The three circles in image (b) mark the positions, which were used to calculate the three exemplary local *I-V* curves shown in figure 5.

(Section 2.3). The regions of high loss current densities of the J_{rec} (550 mV) image correlates with observed cracks in Figure 2 (c) and matches also with the increased J_{02} value by 30.7% in Table II. This proves the observed behaviour of the EL ratio image method with global *I–V* parameters of Section 3.2 that cracks in silicon solar cells increase mainly the global recombination current densities. Furthermore, the induced damage of the mechanical edge isolation machine sample holder is detected in the J_{rec} (550 mV) image of Figure 3 as the same circles, which were seen in the ratio image in Figure 2(c).

To prove the observed influence of cracks on global *I–V* characteristics and whether this influence correlates directly with cracks, local *I–V* characteristics were simulated with the 'Local I-V' tool [5,6]. For this analysis, it is necessary to know the J_{SC} value of the solar cell, which was assumed here to be homogeneous. The resulting images of V_{OC}, FF and η are given in Figure 4. These are images of the local expectation values of V_{OC}, FF, and η, as they would be if the image pixels were electrically isolated from each other.

The V_{OC} image (a) of Figure 4 represents in the yellow (bright) regions a high V_{OC} and in the red (dark) regions a reduced V_{OC}. This also holds for the crack areas and results from the increased recombination by the cracks. The reduced V_{OC} in Figure 4(a) correlates also quite well with the measured decreased V_{OC} values given in Table I.

A similar behaviour is observed for the FF image of Figure 4(b). The regions of cracks are clearly visible and reduce the FF locally; also, the damage of sample holder from the crack formation is visible. These effects are due to a locally increased J_{02}. This FF reduction due to cracks is not so obviously seen in the global *I–V* characteristics data in Table I and demonstrates the need for spatially resolved investigation in the case of local defects.

Finally, the reduced η, which is measured in the global *I–V* characteristics (Table I) can be directly correlated to the cracks by analysing the determined η image of Figure 4(c). The lowest η are observed again for the crack regions. Furthermore, other regions of low η match quite well with losses in the cell by a comparison with the J_{tot} (550 mV) image of Figure 3(b).

After the demonstration of all influences of cracks on the local *I–V* characteristics, the local parameters were averaged over the whole solar cell area to obtain global values for the comparison of the measured global *I–V* characteristics. This comparison demonstrates finally the reliability of the used 'Local I-V' tool to confirm the discussion of crack influences.

In Table III, the measured global *I–V* parameters are listed together with calculated *I–V* parameters from the 'Local I-V' tool except J_{SC}, which is an input parameter of the calculation and therefore identical to the measured value. A direct accordance between measured and

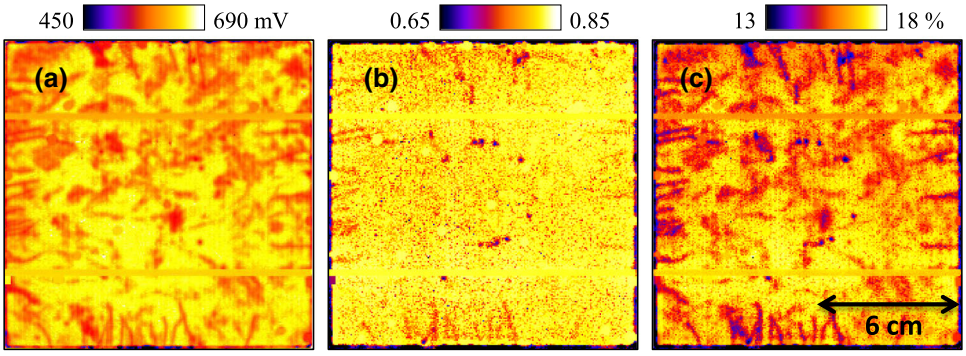

Figure 4. Results of the 'Local I-V' investigation. The image (a) shows a prediction of V_{OC}, the image (b) of FF, and the image (c) of η.

Table III. Comparison of the measured *I–V* parameters and calculated *I–V* parameters from the 'Local I-V' tool.

	V_{OC} (mV)	FF	η (%)
Measured *I–V* characteristics after crack formation	613.5	0.786	15.87
Calculated *I–V* characteristics with 'Local I-V' after crack formation	611.0	0.791	15.90
Absolute (and relative) difference between measured and calculated *I–V* characteristics	−2.5 (−0.4%)	+0.005 (+0.6%)	+0.03 (+0.2%)

Both parameter sets were taken after the crack formation.

calculated values is to be seen for all other parameters in Table III with minor differences, lying in the region of measurement and calculation accuracy. This validates the stability of the calculation method used in this investigation and the assumptions regarding cracks. The different temperature-controlled measurement chucks could be the reason for the small difference of 2.5 mV in V_{OC} due to linear behaviour of V_{OC} and T.

Furthermore, dark and illuminated current density-voltage (*J-V*) curves of three representative positions were extracted from the spatially-resolved 'Local I-V' images to demonstrate the influence of cracks on the *J-V* curve in comparison to non-crack positions. The three selected position for the *J-V* curves are marked in Figure 3 (b) and the corresponding *J-V* curves are illustrated in Figure 5. These *J-V* curves are based on the measurement points (500, 550, 600 mV and −1 V) described in Section 2.3 and calculated with the measured J_{SC} value of 32.9 mA/cm^2 and a fix value of 2 for n_2. Therefore, the exact behaviour for the chosen positions could be slightly different, mainly in the lower voltage range below 400 mV.

In Figure 5 (a), the dark *J-V* curve of the crack position (orange curve) shows over the whole voltage range a higher current density in comparison to a good cell position (green curve). In comparison with a bad cell position (blue curve) there is a difference in the current density mainly in the voltage range below 600 mV. Above 600 mV the curves are nearly identical. The main differences in the *J-V* curve of a crack position in contrast to the two non-crack positions are based on the recombination current density in the depletion region and hence the parameter J_{02}.

Further influences are observed on the illuminated *J-V* curve as well as on the typical solar cell parameters as shown in Figure 5 (b) for the same three positions. The parameters FF, V_{OC} and η are drastically reduced for the cell position with crack in comparison to the two non-crack positions. A decreased η of 1.4 % absolute is observed due to the reduced FF and V_{OC} by the crack. J_{SC} as an input parameter for the calculated illuminated *J-V* curves limited the possibility to estimate the influence of cracks in the voltage range below 400 mV. The main differences between *J-V* curves of the crack and non-crack positions are at around 550 mV, which is exactly the value for the investigation of local currents in Figure 3 and supports therefore the demonstrated influence of cracks on the local *I-V* parameters.

Finally, the global two-diode model values simulated from the 'Local I-V' analysis were compared with that from the evaluation of the measured global *I–V* characteristic. In Section 3.2, all values were calculated with the conventional two-diode model from the measured illuminated *I–V* curve with a constant value of 2 for n_2 and again listed for comparison in Table IV. The same values were calculated with constant n_2 value of 2 as global parameters by averaging the local J_{01}, J_{02} and R_S values of the 'Local I-V' tool calculation and are also listed in Table IV.

The results obtained from the two calculation methods based on different data sets match reasonably well for the parameters (J_{01}, J_{02} and R_S). The obtained values for J_{02}

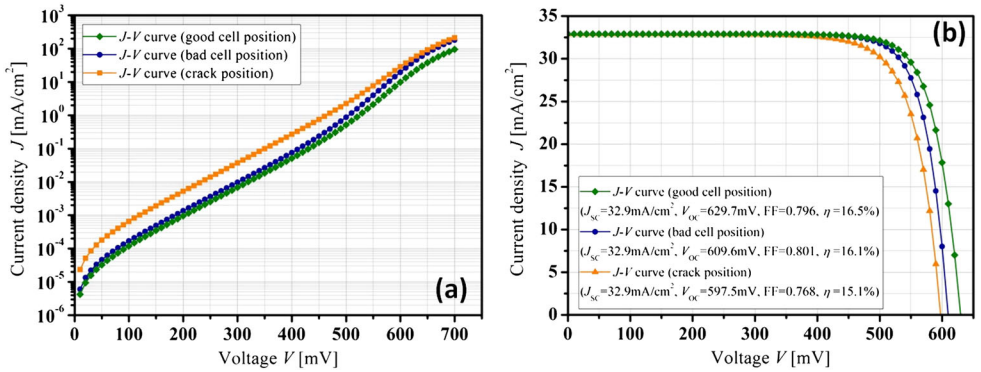

Figure 5. Calculated dark (a) and illuminated (b) *J-V* curves with the "Local I-V" programme for representative positions of the investigated solar cell after crack formation. The selected positions are marked in figure 3 (b). The resultant solar cell parameters for these *J-V* curves are given in the box of figure 5 (b) including the input parameter J_{SC} for the calculation.

Table IV. Comparison of the calculated two-diode model values with conventional model based on the global *I–V* curve and average of the local *I–V* characteristics based on the 'Local I-V' tool.

	J_{01} (pA/cm^2)	J_{02} (nA/cm^2)	R_S (Ωcm^2)
Calculated two-diode model values from the measured global *I–V* curve after crack formation with $n_2 = 2$	1.00	38.7	0.34
Calculated two-diode model values with 'Local I-V' after crack formation with $n_2 = 2$	1.33	39.4	0.37
Absolute (and relative) difference between both methods for the calculation of two-diode model values	+0.33 (+33%)	+0.7 (+1.8%)	+0.03 (+8.8%)

Both calculations were done with constant $n_2 = 2$ in this case.

and R_S are very close to each other, and the differences are in the region of the accuracy of the methods. On the other hand, there is a high relative difference of 33% for the J_{01} value. This difference may stem, for example, from a slightly different temperature of the measurement setups used for the DLIT and *I–V* measurements.

The investigation of the crack influences by the local *I–V* method shows clearly which parameters in the *I–V* characteristics change their behaviour. The main influences of cracks are proven for the recombination current density, but also the diffusion current is slightly increased. Furthermore, with the local *I–V* method, it was possible to demonstrate explicitly for the first time how cracks affected finally the typical *I–V* parameters V_{OC}, FF and η in a detailed investigation.

3.4. Comparison of both imaging methods

The main differences of both imaging methods are the measurement time (seconds for the EL ratio image method and hours for the DLIT local *I–V* method) and the situation that the ratio image method needs an EL image before and after the crack formation or generally at two different times, whereas the local *I–V* method can be used always, when cracks already exist. But a full investigation of crack influences on cells or even modules both methods are beneficial. Furthermore, the local *I–V* method allows a quantitative analysis, whereas the ratio image is a qualitative method, which can be combined with the global *I–V* characteristics. The resolution of the ratio image method is also higher and allows therefore the clearly visible crack detection as it is shown in this paper.

Nevertheless, both methods can also be used separately. In the case of the ratio image method, a cell inspection before and after the module fabrication could be an application to document the crack formation during the module fabrication due to handling or laminating damages. Furthermore, the module inspection itself could be also possible by calculating the ratio image from two EL images, where the first image is taken after the module fabrication and the second image after the module installation in a PV plant or on a roof. This before–after imaging approach allows the documentation of cracks, which were formed by the transport or installation and can increase the annual yield by avoiding defect modules. This approach can also be used by yearly inspection of modules on roofs or in PV plants where the ratio image is calculated from current EL image and previous year's EL image based on a daylight luminescence method published by Stoicescu, *et al.* [13] or by Chunduri, *et al.* [14]. Herewith, the detection of cracks formed by weather influence such as strong wind load or a heavy snow weight is possible and allows an early replacement of defect modules.

In contrast to the ratio image method, the local *I–V* method allows different applications. Overall, the 'Local I-V' tool allows spatially resolved investigation of the two-diode model parameters (J_{PH}, J_{01}, J_{02}, R_S and R_P) and the typical *I–V* parameters (V_{OC}, FF and η) without J_{SC} for every silicon solar cell and is therefore extremely powerful for cell investigation with focus on defects and other local effects. In case of cracks, it is possible to investigate defect cells from the production in an intensive way to find out the influences of cracks or other defects on the cell parameters. This allows a reliable cell and process optimisation concerning yield and efficiency. Furthermore, as shown here, solar cells with cracks, which were detected by the ratio image method, can be investigated in detail by the local *I–V* method.

4. CONCLUSION

This paper presented a detailed analysis of the influence of cracks on the electrical parameter of silicon solar cells in a spatially resolved investigation with two different methods. The local current–voltage analysis of solar cells with cracks shows clearly that cracks mainly affect the recombination current density in the depletion region. This loss current affects further cell parameters such as FF and efficiency, which are confirmed by global current–voltage measurements. The combination of both used techniques, ratio image method and local current–voltage method, allows a complete investigation of cracks in silicon solar cells and their influence. Both methods can be also used separately. The local current–voltage method is more suitable for the cell investigation with a quantitative analysis, whereas the ratio image method is the faster measurement technique, which allows a gradual inspection of cracks on cell and module level.

ACKNOWLEDGEMENTS

The authors thank H. Windgassen and R. Khandelwal from the Institute of Semiconductor Electronics at the RWTH Aachen University to support this work by preparing silicon solar cells. The SEM pictures were carried out by B. Hadam, also from the Institute of Semiconductor Electronics at the RWTH Aachen University, and we thank her for helpful work, as well as U. A. Yusufoglu for the careful reading of the manuscript. The authors are also thankful for the focused ion beam preparation and high resolution SEM pictures, which have been carried out by D. Park from the Central Facility for Electron Microscopy at the RWTH Aachen University.

The work of S. Rißland and O. Breitenstein was financially supported by the German Federal Ministry for the Environment, Nature Conservation and Nuclear Safety and by industry partners within the research cluster 'SolarWinS' (contract No. 0325270C). The content is the responsibility of the authors.

REFERENCES

1. van Mölken JI, Yusufoğlu UA, Safiei A, Windgassen H, Khandelwal R, Pletzer TM, Kurz H. Impact of micro-cracks on the degradation of solar cell performance based on two-diode model parameters. *Energy Procedia* 2012; **27**: 167–172. DOI: 10.1016/j.egypro.2012.07.046
2. Kajari-Schröder S, Kunze I, Eitner U, Köntges M. Spatial and orientational distribution of cracks in crystalline photovoltaic modules generated by mechanical load tests. *Solar Energy Materials and Solar Cells* 2011; **95**(11): 3054–3059. DOI: 10.1016/j.solmat.2011.06.032
3. Fuyuki T, Kondo H, Yamazaki T, Takahashi Y. Uraoka Y. Photographic surveying of minority carrier diffusion length in polycrystalline silicon solar cells by electroluminescence. *Applied Physics Letters* 2005; **86**(26): article 262108. DOI: 10.1063/1.1978979
4. Breitenstein O, Bauer J, Bothe K, Hinken D, Müller J, Kwapil W, Schubert MC, Warta W. Can luminescence imaging replace lock-in thermography on solar cells? *IEEE Journal of Photovoltaics* 2011; **1**(2): 159–167. DOI: 10.1109/JPHOTOV.2011.2169394
5. Breitenstein O. Nondestructive local analysis of current–voltage characteristics of solar cells by lock-in thermography. *Solar Energy Materials and Solar Cells* 2011; **95**(10): 2933–2936. DOI: 10.1016/j.solmat.2011.05.049
6. Breitenstein O. Local efficiency analysis of solar cells based on lock-in thermography. *Solar Energy Materials and Solar Cells* 2012; **107**: 381–389. DOI: 10.1016/j.solmat.2012.07.019
7. Ramspeck K, Bothe K, Hinken D, Fischer B, Schmidt J, Brendel R. Recombination current and series resistance imaging of solar cells by combined luminescence and lock-in thermography. *Applied Physics Letters* 2007; **90**(15): article 153502. DOI: 10.1063/1.2721138
8. Breitenstein O, Khanna A, Augarten Y, Bauer J, Wagner JM, Iwig K. Quantitative evaluation of electroluminescence images of solar cells. *Physica Status Solidi (RRL)* 2010; **4**: 7–9. DOI: 10.1002/pssr.200903304
9. Suckow S, Pletzer TM, Kurz H. Fast and reliable calculation of the two-diode model without simplifications. *Progress of Photovoltaics* accepted and in press. DOI: 10.1002/pip.2301
10. Rißland S, Breitenstein O. Evaluation of luminescence images of solar cells for injection-level dependent lifetimes. *Solar Energy Materials and Solar Cells* 2013; **111**: 112–114. DOI: 10.1016/j.solmat.2012.12.024
11. Steingrube S, Breitenstein O, Ramspeck K, Glunz S, Schenk A, Altermatt PP. Explanation of commonly observed shunt currents in c-Si solar cells by means of recombination statistics beyond the Shockley–Read–Hall approximation. *Journal of Applied Physics* 2011; **110**(1): article 014515. DOI: 10.1063/1.3607310
12. Fuyuki T, Kondo H, Kaji Y, Ogane A, Takahashi Y. Analytic findings in the electroluminescence characterization of crystalline silicon solar cells. *Journal of Applied Physics* 2007; **101**(2): article 023711. DOI: 10.1063/1.2431075
13. Stoicescu L, Reuter M, Werner JH. Daylight luminescence for photovoltaic system testing. Proceedings of the 22nd International Photovoltaic Science and Engineering Conference in Hangzhou/China, 2012
14. Chunduri SK. Out of the dark and into the light. *Photon International* 2012; (11–2012): 126–127.